Online ISSN 1848-3380, Print ISSN 0005-1144
ATKAFF 56(2), 120–131(2015)

Rok Juhant, Darko Vrečko, Jure Knez, Sašo Blažič

Improved Pose Estimation for Vehicle Navigation using Frame Alignment and Forward Smoothing

DOI 10.7305/automatika.2015.04.1051
UDK 681.532.7:007.52; 004.896

Original scientific paper

In this paper we present the application of a modified Extended Kalman filter on a test device. This device is intended to be both rugged and simple to use, providing an accurate position and velocity output for land vehicles. As there are already many applications available for this purpose, our test device is unique in a way that it can be mounted in an arbitrary position on any metal surface on a vehicle, while it automatically discovers its orientation and aligns itself during the first stage of the test period. It comes as an extremely robust and low-cost solution. Furthermore, the pre-alignment outputs are corrected using a reverse output correction during the test period, immediately providing accurate outputs. The alignment algorithm greatly (by factor of 20 or more) reduces the initialization time. In addition, a novel smoothing algorithm with forward computation is described. The developed algorithm is tested with real-world experiments and proved to have a similar accuracy as the reference system, although using much cheaper and less-reliable sensor equipment.

Key words: Alignment, Extended Kalman Filter, GPS/INS Navigation, Smoothing

Poboljšana estimacija položaja za navigaciju vozila koristeći poravnavanje sustava i unaprijedno izglađivanje. U ovome radu opisana je implementacija modificiranog proširenog kalmanovog filtra na testnom uređaju. Uređaj je robustan i jednostavan za upotrebu te omogućava dobivanje točne pozicije i brzine kao izlaznih parametara zemljanih vozila. S obzirom da postoji velik broj postojećih aplikacija, naš testni uređaj je jedinstven u smislu da može biti postavljen u proizvoljnu poziciju na metalnu površinu na vozilu. Uređaj automatski određuje svoju orijentaciju te se poravnava tijekom prvog dijela testnog perioda. Ujedno je vrlo robustan i niske cijene. Izlaz koji se dobije prije poravnavanja ispravljen je koristeći obrnutu korekciju izlaza tijekom testne faze čime se dobiju točni izlazi. Algoritam poravnavanja znatno (za faktor 20 i više) reducira vrijeme potrebno za inicijalizaciju. Opisan je novi algoritam izglađivanja s unaprijednim proračunom. Razvijeni algoritam testiran je na stvarnim podacima te je pokazano da ima sličnu preciznost kao referentni sustav, unatoč korištenju jeftinije i manje pouzdane opreme.

Ključne riječi: poravnavanje, prošireni kalmanov filtar, GPS/INS navigacija, izglađivanje

1 INTRODUCTION

During the development of different applications using the Global Positioning System and Inertial Navigation System (GPS/INS) a lot of solutions have been proposed and many improvements have been made. Researchers have usually focused on different problems that arise when using a vast number of different possible setups of sensors. Usually, GPS sensor and Inertial Measurement Unit (IMU) sensors – gyroscopes and accelerometers – are the basic configuration for land vehicle navigation. However, using these sensors is not the only possible solution. Often other sensors were used to replace GPS or IMU unit. In [1-3], for example, cameras were used instead of GPS to obtain visual information and help calculate the vehicle's position within environment. This approach can also help build the map of the environment with the use of SLAM algorithm which is extremely important at urban places [4] or at places where self-localization is important [5]. Some researchers also used wheel rotational speed sensors [6], laser rangefinder (LRF) sensor [7] or maps of the environment [8]. It is a well-known fact that Micro-electro mechanical sensors (MEMS) are often exposed to high levels of drift. This means that they are quite useless without GPS updates, except when using additional magnetometer sensors. During GPS outages this approach can improve the solution 30 times [9].

All the sensors used in navigation are somehow limited. For a satisfactory solution the errors and limitations must be known and taken care of. GPS signal, for example, can be lost due to different natural (forest, canyon, etc.) or artificial (bridges, high buildings in urban environments, parking garages, etc.) obstructions. MEMS signals, on the

other hand, experience high noise levels and several low-frequency errors. However, the latter is taken into account within the correction part of the filter. These errors are reduced by updating the integration filter (prediction part) with the position and the velocity obtained by the GPS receiver [10]. On the other hand, high-frequency noise (with a particularly significant effect on low-cost units, such as the one, used in our experiments) cannot be effectively filtered using low-pass filters as the filter's cut-off frequency should be lower than the GPS frequency (equal to the reciprocal of the INS working-alone time). This means that the filter's cut-off frequency should be less than 1 Hz, which would mean the loss of important data from the INS signals as shown in [11].

Many studies [12-14] have shown that the errors associated with Gyro sensors (accelerometers and gyroscopes) can be minimized using different methods of off-field calibration. These methods usually take a lot of time (which is also the case with our test reference ADMA-G [1] from Genesys®, which requires 10 seconds of standstill, straight-line acceleration from 0 to 5 m/s and dynamic driving for 120 seconds, which can take nearly 3 minutes of calibration, at best, before starting the measurement, without the installation of hardware being taken into account) and can require additional calibration equipment [15 and 16]. Furthermore, prior calibration cannot remove all the errors, which depend on the testing temperature, the test-track configuration, the method of affixing the sensors to the vehicle, etc.

The greatest and most important part of navigation is a software algorithm. It was shown in [17] that developing a positioning algorithm can be a complex task, involving the use of appropriate estimation techniques and sensor systems for a specific application, and the selection of a suitable algorithm for the navigation. Only with a good positioning solution other tasks, such as Vehicle Routing Problem (VRP) can be taken care of [18].

The majority of algorithms are either completely or partially based on Kalman filter. The basic and widely used approach in terrestrial applications is Extended Kalman filter (EKF) which can give satisfactory results, using a variety of additional approaches to eliminate most common errors. However, in the last few years many different approaches were used, including Unscented or Adaptive Kalman filters which provide better accuracy, especially if the errors change significantly but are potentially unstable compared to EKF [19]. Here some of the most important are mentioned.

In [20] the curve-to-curve matching algorithm after Kalman filtering is described and data fusion using map matching is implemented to correct for the INS drift error. In [21] linear Kalman filters (LKF) were used to determine the trajectory of an athlete executing jumps while skiing, snowboarding, etc. While GPS sensor can give satisfactory results when monitoring the whole track, it lacks in precision at quick changes. This also applies to different land vehicle maneuvers, such as emergency braking, quick turns and full acceleration. This is why accelerometers and gyroscopes are extremely important as can be also concluded from [22], where a hybrid fusion methodology utilizing Dempster-Shafer theory augmented by Support Vector Machines was introduced. This solution can provide accurate results during GPS availability and during GPS outages as well. GPS errors are often the problem when it comes to accuracy, reliability or continuity of position data. This is why sometimes Bayesian filters are used to fuse data from different sensors [23]. It is important that the model of the system is correct as the estimation performance of the Bayesian filters depends on that. As the vehicle model changes with the change of vehicle dynamics during different driving conditions, it is sometimes relevant to use the interacting multiple model (IMM) which adapts to changes of various driving conditions [24]. For GPS denied environments, a centralized or decentralized sensor fusion can be used in the form of dependable navigation, as shown in [25]. It was also shown [26] that sometimes the number of sensors can be reduced without significant changes in accuracy and resulting in much lower costs.

However, each of the mentioned approaches has its downsides, either being computationally very demanding and therefore not adequate for low-cost and mobile units or not low-cost in relation to the equipment used in application. Some were only developed for specific environments (urban areas, snow sports, test tracks with good GPS visibility) or maneuvers (either low or high dynamic). Others were research oriented and could not provide a satisfactory solution for an average user or lack the application of an algorithm and tests in the real world.

Therefore, the features of the proposed solution are the following:

- Low-cost solution, affordable for non-professional use [27], with all the sensors mounted in one case, resulting in robust navigation.

- No additional off-field or on-field calibration for the immediate start of the measurement.

- Use of the EKF algorithm for a stable and computationally undemanding solution.

- General algorithm for all kinds of applications and maneuvers, especially suitable for automotive applications.

- Smoothing algorithm without any additional computational cost.

[1] Datasheet can be obtained at: http://www.genesys-adma.de/adma.php?ID=6935

- Alignment algorithm for arbitrary positioning of a test device.

- All the algorithms are tested on a real device in a real-world environment.

The paper is organized as follows. In next section the hardware of a test device is described. Then, different parts of GPS/INS algorithm, including initialization, prediction and correction, are described. In sections 3.4 and 3.5 a novel smoothing algorithm with forward correction and an alignment algorithm are described, respectively. Then, real-world tests and results are presented. Finally, the most important conclusions are drawn.

2 DESCRIPTION OF THE HARDWARE

We tried to develop a system that would be as autonomous and simple to use as possible. A plug-in was created that receives the data from all the sensors – global positioning system (GPS) and inertial measurement unit (IMU) – and calculates the outputs. The test device (referred to as Gyro in the following) used in the experiments consists of a small MEMS accelerometer and gyroscope unit ADIS 16400[2], a GPS receiver CW25[3] and has an integrated GPS antenna. It is implemented in the form of a strap-down arrangement [28].

The sensors were put in an aerodynamic, waterproof, plastic (allowing the GPS signal to be uninterrupted) box with three magnets in the base for fixing it to the roof of the vehicle (Fig. 1).

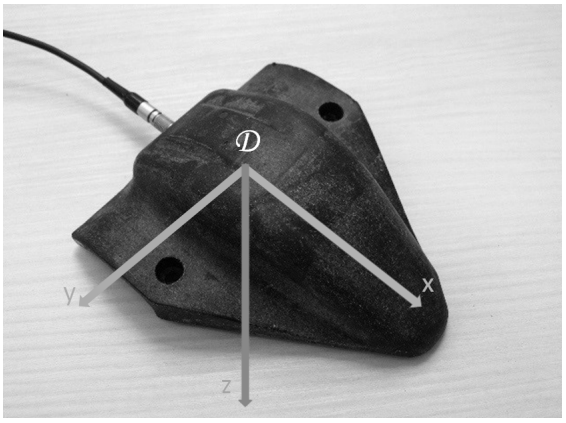

Fig. 1. Test device (Gyro) with GPS and inertial sensors and its own coordinate system

This unit is very small (120 mm × 110 mm × 40 mm) and light (220 g). Its sensors output six parameters of inertial data (the acceleration and the angular velocities in three axes) with a 768-Hz sample rate and six parameters of GPS data (longitude - λ, latitude - φ, altitude - h, number of visible satellites - S_v, velocity - v and heading - ψ) with a 1-Hz sample rate. The serial data connection and power involve a 4-pin Controller Area Network (CAN) cable connector. The data sent from the Gyro device is stored and processed by a measurement device.

The GPS receiver used in our tests, though being inexpensive, was designed especially for weak-signal environments. In reality, the quality of the GPS outputs depends on the speed of the vehicle (when stationary the GPS system cannot determine the heading and also the positional error is relatively large) and the number of visible satellites (more satellites results in a better accuracy). A demonstration of this statement can be seen in Fig. 2, where the static accuracy of the GPS sensor is shown. While dynamic error of GPS data is typically less than 10 m, the static error can be more than 50 m.

Fig. 2. Static GPS error during a 3-hour test

3 DESCRIPTION OF GPS/INS ALGORITHM

For a better understanding of the algorithm, first the coordinate systems used in this paper and the relations between them are presented. The world geodetic system (WGS84) is a standard, Cartesian, right-handed coordinate system used for GPS data. Its axes are longitude, latitude, – in radians, and altitude – height above the sea level – in meters. The navigation coordinate system (NED), which is very similar to WGS84, is a geodetic system. The axes (in meters) are x (north), y (east) and z (down). The NED coordinate system and WGS84 are presented in Fig. 3 and are linearly connected. The NED frame is the main frame in our study, since all the outputs are given in it. It was chosen because it has the most intuitive representation of the navigation data.

The body frame is presented in Fig. 4. Its center and axes are aligned with the car. If the vehicle were to move

[2]Datasheet can be found at: http://www.analog.com/en/index.html
[3]Datasheet available at: http://www.navsync.com

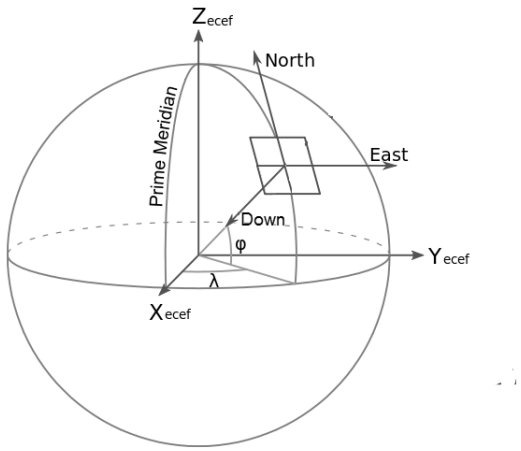

Fig. 3. NED and WGS84 coordinate system

forward, x would point in the direction of travel and the z axis would point towards the centre of the Earth.

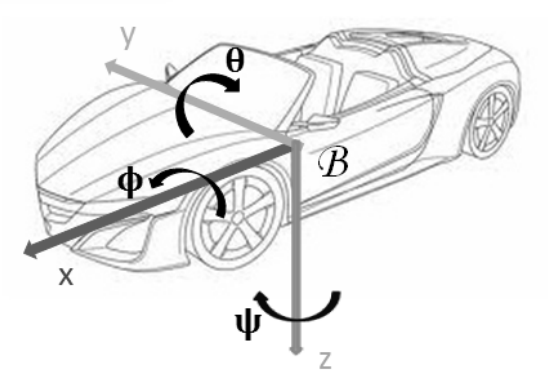

Fig. 4. Body coordinate system

As was already mentioned, the Gyro device can be mounted at an arbitrary angle on the surface of the vehicle. This means that the body and the device (shown in Fig. 1) coordinate systems are not necessarily aligned. If the device is installed on a flat, level surface, the x axis is pointing forward, the y axis is pointing right and the z axis is pointing downwards. The alignment procedure is described in Section 3.5.

To obtain the position and velocity from the Gyro test device, first the initial position must be known. Then each time inertial data ($\mathbf{a}^b = \begin{bmatrix} a_x^b & a_y^b & a_z^b \end{bmatrix}^T$ is a vector of the accelerations in the body frame and $\omega^b = \begin{bmatrix} \omega_x^b & \omega_y^b & \omega_z^b \end{bmatrix}^T$ is a vector of the turn rates in the body frame) arrive, the prediction step of the Kalman filter is executed.

The system operation can be divided into three stages. The first stage is a determination of the initial values and the alignment. The second stage is normal operation, which can be divided into two modes. The first mode of the second stage (default) is the operation with GPS measurements available (Fig. 5). Second mode of the second stage is operation with GPS measurements unavailable, which means that only Gyro measurements are used (the prediction stage of the Kalman filter). The third stage begins when the alignment is finished. During the third stage (which runs simultaneously with the second stage) the prior outputs are calculated with the alignment values taken into account. This technique enables us to obtain all the data from the beginning of the measurement as if they were all measured with calibrated, un-biased and aligned sensors. This stage could be carried out in post-production, but the used measurement software allows us to calculate the outputs during the measurement, making the system interesting for the control of vehicles [29] and [30].

3.1 Initialization

During initialization procedure the determination of initial values is performed. Since the alignment is made afterwards, the initial values are determined as if the vehicle is level with a flat surface.

At the start of the measurement (standstill) the GPS data, i.e., initial longitude, latitude, altitude, velocity and vertical velocity, and the IMU data, i.e., initial accelerations $\mathbf{a}_0^b$ and turn rates $\boldsymbol{\omega}_0^b$, are determined by averaging. The initial heading cannot be exactly defined at standstill (i.e., with the GPS velocity being less than 0.5 m/s) and is determined later, when the vehicle starts to move. At least one GPS sample is needed for a successful initialization, while the number of INS data needs to be much higher. This is because the INS data contain a lot of noise and averaging gives better results.

The initial roll (ϕ) and pitch (θ) angles in the NED frame can be determined with the use of elements of the Direction Cosine Matrix(DCM). The yaw angle - direction (ψ) cannot be determined until the vehicle starts to move.

The covariance matrices for the Gyro and GPS outputs are determined during initialization (standstill), because their values can vary from one test cycle to another.

The noise covariance matrix of the Gyro measurements for the normal operational mode can be written as

$$\mathbf{Q} = \mathrm{diag}(\sigma_{ax}^2,\, \sigma_{ay}^2,\, \sigma_{az}^2,\, \sigma_{\omega x}^2,\, \sigma_{\omega y}^2,\, \sigma_{\omega z}^2), \qquad (1)$$

where σ denotes the standard deviation of each measurement. The variance values are calculated during the initialization (at standstill) using a statistics formula integrated

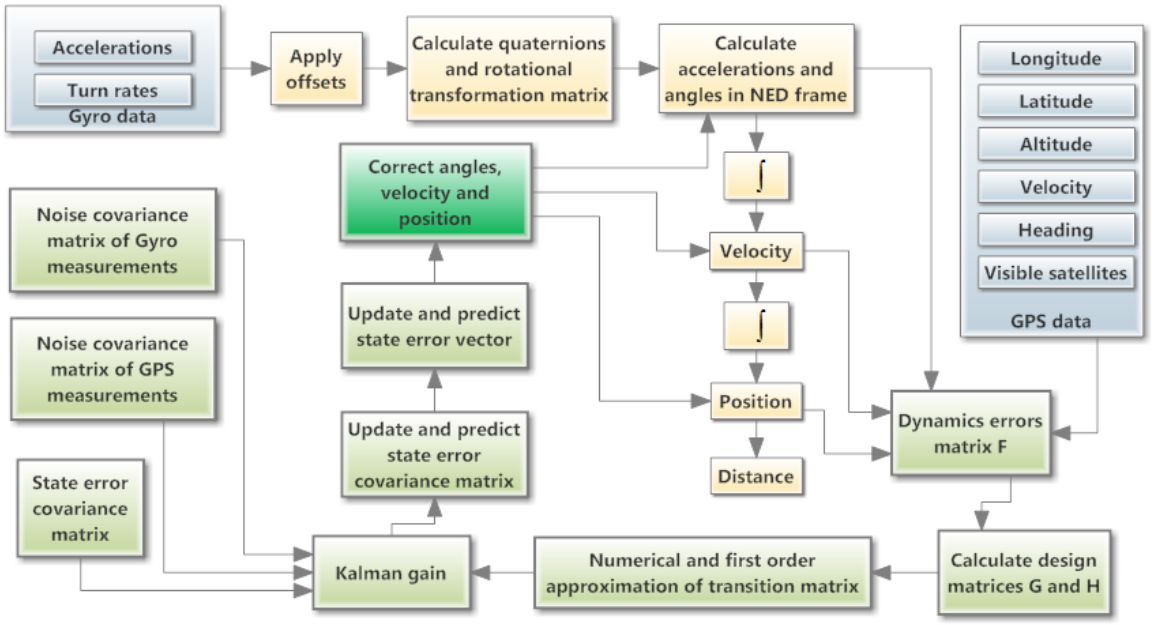

Fig. 5. Block diagram of a system during the first mode of the second stage

into the measurement software. The following formula for a variance determination in a discrete system is used:

$$\sigma^2 = \frac{1}{k_{st}} \sum_{k=0}^{k_{st}} (x_k - \overline{x})^2, \tag{2}$$

where x_k denotes the current (last) accelerometer, gyroscope or GPS value and $\overline{x}$ denotes the average of the corresponding signal. Typical values for the acceleration standard deviations σ_{ax}, σ_{ay} and σ_{az} during the test were 0.22 m/s, while the gyroscope standard deviations $\sigma_{\omega x}$, $\sigma_{\omega y}$ and $\sigma_{\omega z}$ were 3.50·10-3 rad/s.

3.2 Prediction

Each time new Gyro data arrive (768-Hz sample rate), the position and the velocity are calculated. This also serves as a prediction part of the Kalman filter. All the input inertial variables are first transformed from the body frame to the NED frame using quaternions and transformation matrix DCM. After that velocity is calculated using the backward differentiation formula. The position in the WGS84 frame is calculated using the trapezoidal method.

3.3 Correction

The GPS data are received with a significantly smaller sample rate than the INS data and are used as a correction part in the Kalman filter. Correction part of our algorithm is based on a nine-state Kalman filter (position, velocity and rotations), presented in [16], and modified in a way to comply with our system.

The noise covariance vector of the GPS measurements needs to be determined. It can be defined as

$$\mathbf{R} = \mathrm{diag}\left(\sigma_{\varphi}^2,\ \sigma_{\lambda}^2,\ \sigma_{h}^2,\ \sigma_{vn}^2,\ \sigma_{ve}^2,\ \sigma_{vd}^2,\ \sigma_{vy}^2,\ \sigma_{vz}^2\right). \tag{3}$$

The non-holonomic constraints are related to the assumption that the vehicle's velocity in the plane perpendicular to the forward direction (left-right and up-down) is almost zero. This is why the variables σ_{vy} and σ_{vz} from equation (3) are used as measurement updates for the Kalman filter. They can be calculated with the use of cosine transformation matrix as:

$$\mathbf{v}^b = \mathbf{C}^T \mathbf{v}^n, \tag{4}$$

where $\mathbf{v}^b = \begin{bmatrix} v_x & v_y & v_z \end{bmatrix}^T$ and $\mathbf{v}^n = \begin{bmatrix} v_N & v_E & v_D \end{bmatrix}^T$ denote the velocity in the body and the navigation frame, respectively, and $\mathbf{C}$ is the DCM matrix.

As the accuracy of the GPS values also depends on the number of visible satellites, an additional factor, defined as $w = 1/S_v$ (where S_v denotes number of visible satellites), for the GPS variance's weight is introduced.

Experiments have shown that for more than four visible satellites the noise covariance vector can be defined as:

$$\mathbf{R} = w \cdot \mathrm{diag}\left(10,\ 10,\ 20,\ 0.1,\ 0.1,\ 0.1,\ 10,\ 10\right). \tag{5}$$

If the number of visible satellites is less than four (not enough satellites for a position and velocity determination), the elements of the noise covariance matrix of the GPS measurements have the following values

$$\mathbf{R} = \mathrm{diag}\,(100,\ 100,\ 200,\ 1,\ 1,\ 1,\ 0.01,\ 0.01)\,. \quad (6)$$

3.4 Smoothing

The error state vector is used to correct the accelerations, turn rates, velocities and positions that will be used for subsequent prediction steps. During 767 prediction steps without correction (note: 768-Hz Gyro rate and 1-Hz GPS rate) the position and velocity can experience such drift that the correction produces significant changes in the output signals. Therefore, it is common to use different computationally challenging smoothing methods, for example, factor graph-based incremental smoothing as proposed by [31]. Our algorithm (forward smoothing), in contrast, uses the error state vector to incrementally correct the calculated outputs. This means that instead of correcting the output signals only once after each correction cycle, they are also corrected 767 times during each prediction cycle. Using this approach resulted in smooth output values and no additional processor load. For smoothing purposes a new variable is introduced. This variable can correct for special cases, which can occur between two cycles of correction. It can be explained with a simple example.

If a vehicle was to accelerate from one to another cycle of correction (from correction sampling instant $(j-1)$to j) and the prediction velocity $v_{INS}(j)$ at sampling instant j was to be smaller than $v_{GPS}(j)$, then the state error vector would tend to correct the velocity with positive velocity correction factors. If then after prediction between sampling instants j and $(j+1)$ the velocity v_{INS} would start to decrease, it would still be corrected with positive state error vector factors. In this case it is better to decrease the contribution of the state error correction factor. This idea is used for all variables that are corrected with the state error vector (position, velocity and rotation). Our implementation of this idea is explained with the following equations.

The change factor vector can be defined as:

$$\mathbf{c} = \begin{bmatrix} \mathbf{c}_r & \mathbf{c}_v & \mathbf{c}_\epsilon \end{bmatrix}^T, \quad (7)$$

where $\mathbf{c}_r = \begin{bmatrix} c_\varphi & c_\lambda & c_h \end{bmatrix}^T$, $\mathbf{c}_v = \begin{bmatrix} c_{vn} & c_{ve} & c_{vd} \end{bmatrix}^T$ and $\mathbf{c}_\epsilon = \begin{bmatrix} c_\phi & c_\theta & c_\psi \end{bmatrix}^T$.

Considering the above equation, the position during the prediction is calculated using the modified equation from [16]:

$$\begin{aligned}\mathbf{r}^n(k) =& \mathbf{r}^n(k-1) + 0.5\mathbf{D}^{-1}(k)\,(\,\mathbf{v}^n\,(k) \\ &+ \mathbf{v}^n(k-1)\,)\,\Delta t_{INS} - \mathbf{c}_r\delta\mathbf{r}^n,\end{aligned} \quad (8)$$

where

$$\mathbf{D}^{-1}(k) = \begin{bmatrix} \frac{1}{R_N+h} & 0 & 0 \\ 0 & \frac{1}{(R_E+h)cos\lambda} & 0 \\ 0 & 0 & -1 \end{bmatrix} \quad (9)$$

and $\mathbf{r}^n(k) = \begin{bmatrix} \varphi & \lambda & h \end{bmatrix}$. R_N and R_E are north and east radii of curvature, respectively, $\mathbf{v}^n(k)$ and $\mathbf{v}^n(k-1)$ are the current and previous velocity in the NED frame, respectively, Δt_{INS} is the interval between the previous and the current (last) Gyro sample and can be expressed as $\Delta t_{INS} = t(k) - t(k-1) = 1/f_{INS}$, where f_{INS} is the frequency of inertial data.

The velocity during the prediction is calculated using following modified equation:

$$\mathbf{v}^n(k) = \mathbf{v}^n(k-1) + \dot{\mathbf{v}}^n(k)\Delta t_{INS} - \mathbf{c}_v\delta\mathbf{v}^n, \quad (10)$$

where $\dot{\mathbf{v}}^n(k)$ denotes the time derivative of the velocity.

The matrix $\mathbf{C}$ can be corrected during the prediction using the equation:

$$\mathbf{C}_c = \begin{bmatrix} 1 & -c_\theta\epsilon_D & c_\phi\epsilon_E \\ c_\theta\epsilon_D & 1 & -c_\psi\epsilon_N \\ -c_\phi\epsilon_E & c_\psi\epsilon_N & 1 \end{bmatrix}\mathbf{C}, \quad (11)$$

where $\epsilon^n = \begin{bmatrix} \epsilon_N & \epsilon_E & \epsilon_D \end{bmatrix}^T$ is an attitude error vector.

There are two options for the coefficients of the change factor vector, as explained above. Let us give the equation for the determination of the longitude change factor:

$$c_\lambda = \begin{cases} \frac{1}{f_{INS}}, & \lambda_{diff}\delta\lambda \geq 0, \\ \frac{1}{f_{INS}(1-b)}, & \lambda_{diff}\delta\lambda < 0, \end{cases} \quad (12)$$

where $\lambda_{diff} = \lambda_k - \lambda_{k-1}$ and $b = \mathrm{sign}(\delta\lambda)\lambda_{diff}$. $\delta\lambda$ is the first element of the error state vector, expressed as $\mathbf{x} = \begin{bmatrix} \delta\mathbf{r}^n & \delta\mathbf{v}^n & \epsilon^n \end{bmatrix}^T$, where $\delta\mathbf{r}^n = \begin{bmatrix} \delta\varphi & \delta\lambda & \delta h \end{bmatrix}^T$, $\delta\mathbf{v}^n = \begin{bmatrix} \delta v_N & \delta v_E & \delta v_D \end{bmatrix}^T$ and $\delta\mathbf{r}^n = \begin{bmatrix} \delta\phi & \delta\theta & \delta\psi \end{bmatrix}^T$. Equations, analogue to (12), can be applied for all coefficients of a change vector. The improvement in the output signals when using this approach is shown in Section 4.2.

3.5 Frame Alignment

Let us assume that we have two different GPS locations at sampling times $t(k)$and $t(k+1)$. At time $t(k)$ we start calculating the outputs with the Gyro device. If the device and body (car) coordinate system were to be aligned, then the position $\mathbf{r}'_2$ at $t(k+1)$, calculated from the accelerometers and gyroscopes, would be the same as the GPS position ($\mathbf{r}_2$). Since the coordinate systems are not necessarily aligned, the positions would generally be

different, as can be seen in Fig. 6. Although the angle $\alpha = \begin{bmatrix} \alpha_x & \alpha_y & \alpha_z \end{bmatrix}$ consists of three angles in three planes, in this visual example the Gyro device is rotated by an angle of 90° in one plane (for a simple illustration only the 1D angle is used), which means that the y-axis points in the direction of the car's movement instead of the x-axis. If then between two GPS data the vehicle (body) was to move forward in the x direction from point R_1 to point R_2, in the device coordinate system, that would be a movement in the y direction. After the transformation using matrix $\mathbf{C}$, this would result in a movement perpendicular to the actual change of position.

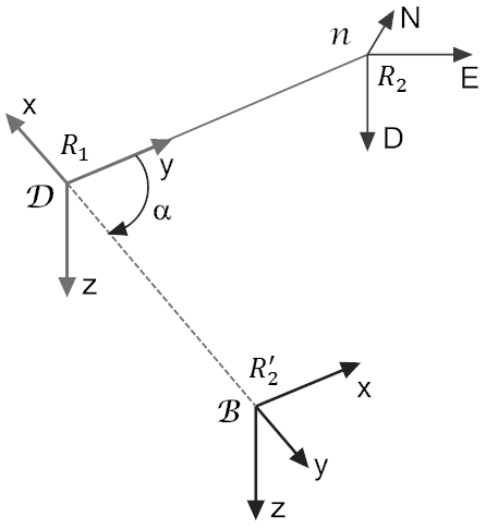

Fig. 6. Demonstration of different coordinate systems and alignment method

Let us define two vectors: $\vec{r_t} = \vec{R_1 R_2}$ and $\vec{r_c} = \vec{R_1 R_2'}$. In order to calculate the misalignment between the body and the device coordinate system, we need to determine an angle α between those two vectors, which involves a separate calculation of three angles using the scalar product of the vectors $\vec{r_c}$ and the projection of a vector $\vec{r_t}$, denoted as $\vec{r_p}$. All the calculations are made with respect to the body coordinate system. The angle α_x can be calculated with the following formula:

$$\alpha_x = \arccos\left(\frac{\vec{r_c}\cdot\vec{r_p}}{\left\|\vec{r_c}\right\|\cdot\left\|\vec{r_p}\right\|}\right)\Bigg|_{zx}, \qquad (13)$$

where zx denotes the plane to which the vector $\vec{r_t}$ is projected. Analogous formulas can be applied to calculate α_y (with a projection to the xy plane) and α_z (with a projection to the yz plane).

After the angles are determined, they need to be applied during the next prediction step. This is done with rotational matrix, defined as

$$\mathbf{R} = \mathbf{R}(\alpha_x)\,\mathbf{R}(\alpha_y)\,\mathbf{R}(\alpha_z), \qquad (14)$$

where $\mathbf{R}(\alpha_x)$ is a rotational matrix about the x-axis, $\mathbf{R}(\alpha_y)$ is a rotational matrix about the y-axis and $\mathbf{R}(\alpha_z)$ is a rotational matrix about the z-axis of a device coordinate system. The accelerations and turn rates can now be converted from the device to the body coordinate system at the beginning of each prediction step. The alignment procedure is calculated after every correction step until sufficient accuracy is achieved. Usually, it takes up to 30 correction cycles to successfully align the device and the body coordinate system.

Note that the alignment procedure (calculation of the angles) is performed only when the number of GPS satellites is sufficient (six or more) to prevent large errors.

3.6 Pre-alignment correction

When the alignment procedure is finished, the outputs from the beginning of the test to the end of the alignment procedure need to be corrected. In this phase of the development the calculation is performed using the standard procedures, described in Sections 3.2 and 3.3. The drawback of this method is the discontinuity that can occur at the border between the end of the alignment and the beginning of the normal calculation mode. This can be overcome by the use of smoothing.

4 TESTING AND RESULTS

Various tests have been made at different stages of the algorithm's development. The initial tests indicated the direction in which the algorithm needed to be improved. Some tests were performed using a 20-Hz GPS sensor that was built in a logging device.

The proposed system is denoted as Gyro and its data is compared to the ADMA-G reference device. Data of a raw GPS data is also shown to demonstrate the quality of the signals used as correction in our system.

4.1 Normal operation mode

The first test was made to show the filtering of the Kalman algorithm during the normal operating mode. Initialization and alignment were already completed. The test was made with a 20-Hz GPS receiver.

Figure 7 shows the position filtering during the 30-second test. The plus signs represent the initial positions.

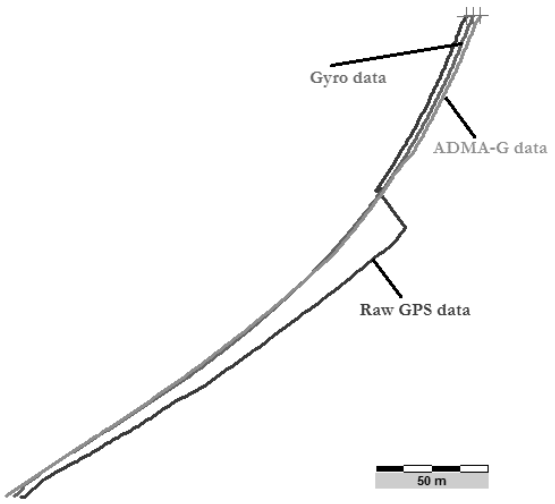

Fig. 7. Position filtering during a short test period

The raw position from the GPS sensor jumps by 20 m in the middle of the test, but our algorithm (Gyro data) manages to keep the output trajectory smooth. The second example in Fig. 8 shows some velocity filtering, which was made during a 3-second test. It is clear that the velocities of the ADMA-G and the Gyro are almost the same, while the GPS velocity has a lot of noise and error.

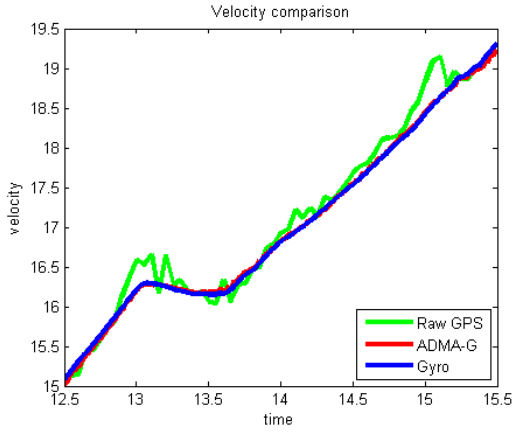

Fig. 8. Velocity filtering during a short test period

4.2 Smoothing algorithm

The novel smoothing algorithm was tested several times during the development. The improvements made using this algorithm can be demonstrated with a turn section of a road, as shown in Fig. 9. The raw GPS data can clearly be seen to have only a 1-Hz update rate, as the curve is not smooth. The orange (Gyro system) and violet (reference system) curves are completely overlapped, with the largest difference of 0.12 m between the positions. This is why an orange curve is practically not seen on this figure. The blue and yellow curves show examples of over- and under-sized change factors for latitude and longitude, respectively. When the proposed smoothing algorithm was used, the accuracy of the system improved greatly. The errors were decreased by a factor 10 (2 m error without and 0.2 m error with smoothing algorithm).

4.3 Alignment

In this paragraph an example of an improvement using the alignment method and the pre-alignment correction will be presented. In this test the GPS module was rotated by 30 degrees around y -axis and 10 degrees around x -axis of the body coordinate system. An alignment algorithm discovered the orientation of the device with typical accuracy of less than 2° for all the angles (roll, pitch and jaw), often even under 1°. Better accuracy is limited by the noise and drift of the inertial signals.

A graphical representation is shown in Fig. 10. It is evident that the aligned Gyro and ADMA-G outputs are similar. The maximum difference between them is only 0.3 m, except for the start of the measurement, where the ADMA-G output is absent (15 seconds) due to the lack of visible satellites. However, the aligned Gyro's better GPS receiver (for low signal environments) provides sufficient data. The unaligned Gyro, on the other hand, does not manage to provide an accurate output, despite the GPS corrections.

Another advantage of the alignment algorithm is a short time needed for initialization of the system. Most existing methods need one minute at least to start the measurement while our method reduces that time to a few seconds at most cases. This means an improvement by factor 20 or even more.

The tests have shown that even though the covariance vector often changes (the number of visible satellites was typically between 5 and 8) and its change is abrupt (see Section 3.3), this does not have any significant or noticeable effect on the stability of the Gyro system.

5 CONCLUSION

During the development of the Gyro test system (hardware and software) we experienced many different challenges. We succeeded in our initial goal to develop a system that would require the minimum possible initialization procedure. With the help of the measurement software implemented we managed to almost eliminate the standard initialization procedure. The user of our system, which is

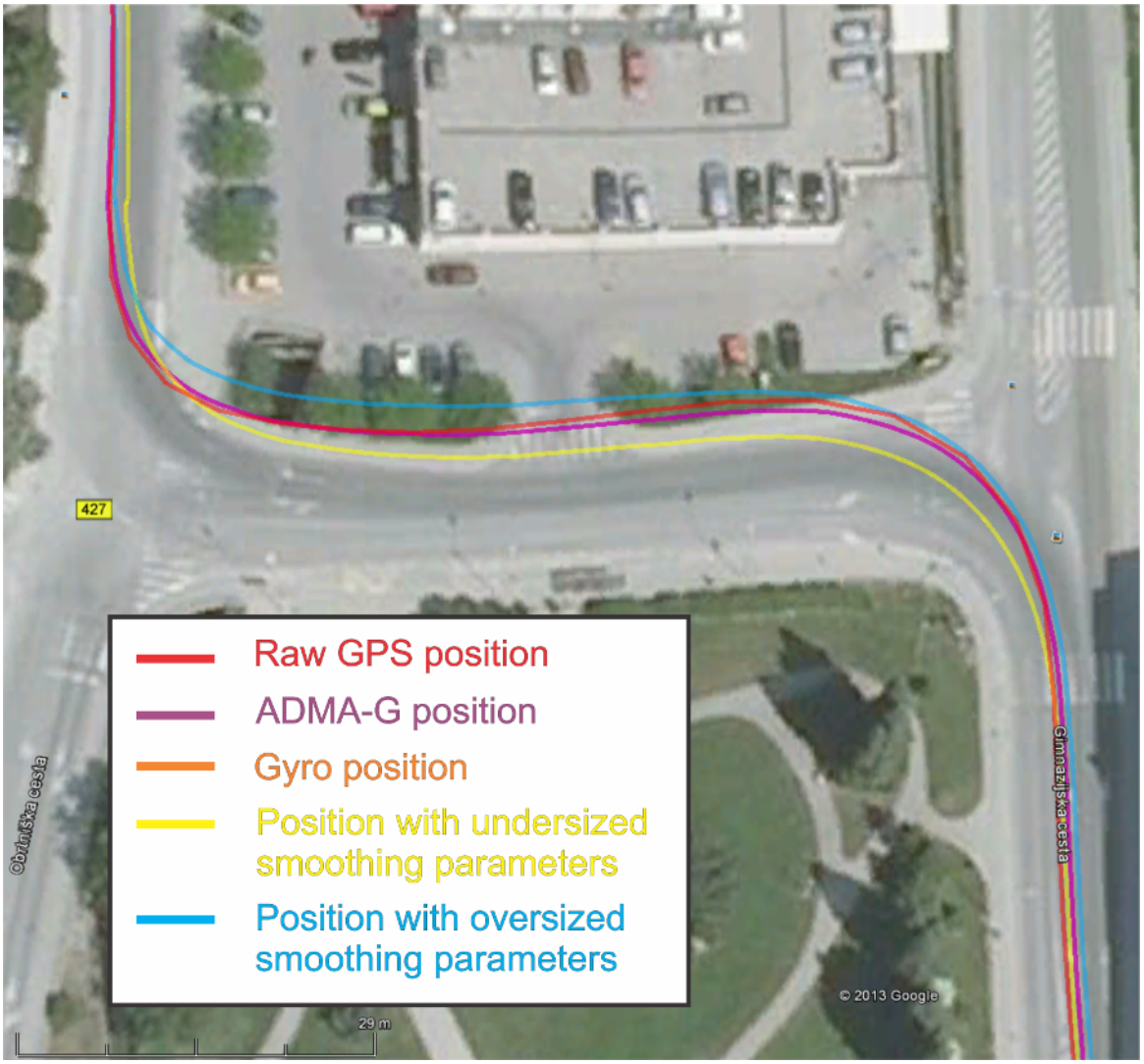

Fig. 9. Visual representation and evaluation of smoothing algorithm

still under development, will be able to start the test procedure almost immediately. Our newly developed alignment procedure is also a step forward in terms of reducing the user's work. The device can be optionally mounted on the surface of the vehicle and its orientation is discovered with the error of less than 2° of roll/pitch/jaw angles.

The novel smoothing method with no backward calculation proved to be simple but effective. Moreover it requires no extra load on the processor, which will be useful for further development. The position accuracy improved from around 2 m without using a smoothing method to less than 0.20 m during tests.

The next revisions of the test device will focus on optimization of the algorithm calculation. Special care will be taken to determine other sensor errors using the described alignment procedure. Our main goal for the future is an even more robust device with a battery and processor inside the Gyro test device. The aim will also be to improve the software algorithm to achieve better results with the same level of accuracy for the GPS and inertial sensor.

ACKNOWLEDGMENT

Operation part financed by the European Union, European Social Fund.

The authors would like to thank people at Dewesoft for providing relevant support.

REFERENCES

[1] D. D. Diel, P. DeBitetto, S. Teller, "Epipolar Constraints for Vision-Aided Inertial Navigation," *Pro-*

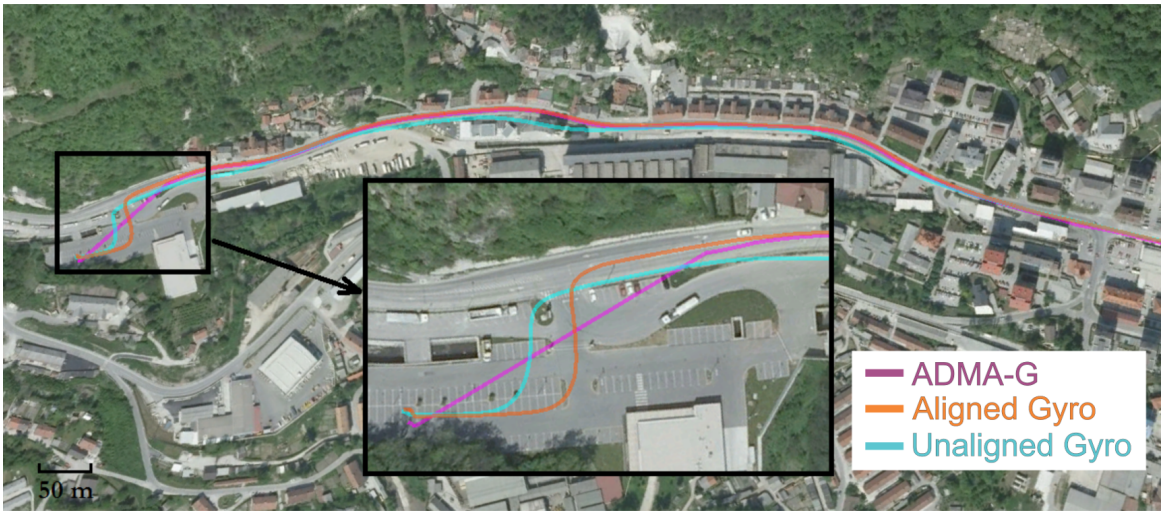

Fig. 10. Improvement using alignment method and pre-alignment correction

ceedings of the Seventh IEEE Workshops on Application of Computer Vision, (Breckenridge, CO), January 2005.

[2] J. Hol, *Sensor Fusion and Calibration of Inertial Sensors, Vision, Ultra-Wideband and GPS*. PhD thesis, Linköping University, 2011.

[3] A. Mourikis, S. Roumeliotis, "A Multi-State Constraint Kalman Filter for Vision-aided Inertial Navigation," *Proceedings of the 2007 IEEE International Conference on Robotics and Automation*, (Rome, Italy), April 2007.

[4] J. Kim, S. Sukkarieh, "SLAM aided GPS/INS Navigation in GPS Denied and Unknown Environments," *Proceedings of the 2004 International Symposium on GNSS/GPS*, (Sydney, Australia), December 2004.

[5] E. Ivanjko, A. Kitanov, I. Petrović, *Model based Kalman Filter Mobile Robot Self-Localization*, HanafiahYussof (Editor), Robot Localization and Map Building. In-Tech, Vukovar, Croatia, pp. 59-89, 2010.

[6] J. Gao, M.G. Petovello, M.E. Cannon, "Development of Precise GPS/INS/Wheel Speed Sensor/Yaw Rate Sensor Integrated Vehicular Positioning System," *Proceedings of the 2006 National Technical Meeting of The Institute of Navigation*, (Monterey, CA), January 2006.

[7] L. Teslić, I. Škrjanc, G. Klančar, "Using a LRF sensor in the Kalman-filtering-based localization of a mobile robot," *ISA Transactions*, vol. 49, no. 1, pp. 145-153, 2010.

[8] S. Syed, E. Cannon, "Map-Aided GPS Navigation: Linking Vehicles and Maps to Support Location-Based Services," *GPS World*, vol. 16, no. 11, pp. 39-44, 2005.

[9] O. J. Woodman, "An introduction to inertial navigation," technical report, University of Cambridge, Cambridge, 2007.

[10] J. Skaloud, *Optimizing Georeferencing of Airborne Survey Systems by INS/DGPS*. PhD thesis, University of Calgary, 1999.

[11] Y. Ban, Q. Zhang, X. Niu, W. Guo, H. Zhang, J. Liu, "How the Integral Operations in INS Algorithms Overshadow the Contributions of IMU Signal Denoising Using Low-Pass Filters," *Journal of Navigation*, vol. 66, pp. 837-858, 2013.

[12] V. Krishnan, K. Grobert, "Initial alignment of a gimballess inertial navigation system," *IEEE Transactions on Automatic Control*, vol. 15, no. 6, pp. 667-671, 1970.

[13] F. Sun, T. Cao, B. Xu, Y. Ben, Y. Wang, "Initial alignment for strapdown inertial navigation system based on inertial frame," *Proceedings of the 2009 International Conference on Mechatronics and Automation*, (Changchun, China), August 2009.

[14] Z. Wu, Z. Wang, Y. Ge, "Gravity based online calibration for monolithic triaxial accelerometers' gain and offset drift," *Proceedings of the 4th World Congress on Intelligent Control and Automation*, (Shanghai, China), June 2002.

[15] I. Frosio, F. Pedersini, N. A. Borghese, "Autocalibration of MEMS Accelerometers," *IEEE Transactions on Instrumentation and Measurement*, vol. 58, no. 6, pp. 2034-2041, 2009.

[16] E.-H. Shin, *Accuracy Improvement of Low Cost INS/GPS for Land Applications*. Master Thesis, University of Calgary, 2001. Available at: http://oleate.free.fr/Doc_Inge/Theses/2001%20SHIN%20-%20Accuracy%20Improvement%20of%20Low%20Cost%20INS-GPS%20for%20Land%20Applications.pdf

[17] J. Lozano, L. Carrillo, A. Dzul, R. Lozano, "Spherical simplex sigma-point Kalman filters: A comparison in the inertial navigation of a terrestrial vehicle," *Proceedings of the American Control Conference*, (Seattle, WA), June 2008.

[18] J. Fosin, T. Carić, E. Ivanjko, "Vehicle Routing Optimization Using Multiple Local Search Improvements," *Automatika*, vol. 55, no. 2, 2014.

[19] C. Hide, T. Moore, M. Smith, "Adaptive Kalman Filtering for Low-cost INS/GPS," *The Journal of Navigation*, vol. 56, pp. 143-152, 2003.

[20] H.-J. Chu, G.-J. Tsai, K.-W. Chiang, T.-T. Duong, "GPS/MEMS INS Data Fusion and Map Matching in Urban Areas," *Sensors,* vol. 13, no. 9, pp. 11280-11288, 2013.

[21] F. Sadi, R. Klukas, "New Jump Trajectory Determination Method using Low-Cost MEMS Sensor Fusion and Augmented Observations for GPS/INS integration," *GPS Solutions*, vol. 17, no. 2, pp. 139-152, 2013.

[22] D. Bhatt, P. Aggarwal, V. Devabhaktuni, P. Bhattacharya, "A Novel Hybrid Fusion Algorithm to Bridge the Period of GPS Outages using Low-Cost INS," *Expert Systems with Applications,* vol. 41, no. 5, 2014.

[23] I. Marković, I. Petrović, "Bayesian Sensor Fusion Methods for Dynamic Object Tracking – A Comparative Study," *Automatika (in press)*, 2014.

[24] K. Jo, K. Chu, M. Sunwoo, "Interacting Multiple Model Filter-Based Sensor Fusion of GPS With In-Vehicle Sensors for Real-Time Vehicle Positioning,", *IEEE Transactions on Intelligent Transportation Systems*, vol. 13, no. 1, pp. 329-343, 2011.

[25] M. Illyas, K. Cho, S. Park, S.-H. Baeg, "Dependable Navigation in GPS Denied Environment: A Multi-Sensor Fusion Technique," *Proceedings of 44th International Symposium on Robotics (ISR)*, (Seoul, S. Korea), October 2013.

[26] N. El-Sheimy, "The Potential of Partial IMUs for Land Vehicle Navigation," *InsideGNSS*, vol. Spring 2008, pp. 16-25, 2008.

[27] K. J. Walchko, M. C. Nechyba, E. Schwartz, A. Arroyo, "Embedded Low Cost Inertial Navigation System," in *Proceedings of the Florida Conference on Recent Advances in Robotics*, (Dania Beach, FL), May 2003.

[28] S. Sukkarieh, *Low Cost, High Integrity, Aided Inertial Navigation Systems for Autonomous Land Vehicles*. PhD thesis, The University of Sydney, 2000.

[29] J. Yang, E. Hou, M. Zhou, "Front Sensor and GPS-Based Lateral Control of Automated Vehicles," *IEEE Transactions on Intelligent Transportation System*, vol. 14, pp. 146-154, 2013.

[30] C. Pozna, F. Troester, R.-E. Precup, J. K. Tar, S. Preitl, "On the design of an obstacle avoiding trajectory: Method and simulation," *Mathematics and Computers in Simulation*, vol. 79, pp. 2211-2226, 2009.

[31] V. Indelman, S. Williams, M. Kaess, F. Dellaert, "Information fusion in navigation systems via factor graph based incremental smoothing," *Robotics and Autonomous Systems*, vol. 61, no. 8, pp. 721-738, 2013.

Rok Juhant received his B.Sc. degree in 2010 from the Faculty of Electrical Engineering, University of Ljubljana. His B.Sc. thesis was the subject of a patent application. He is currently a young researcher at Dewesoft, Slovenia. His current and past research interests include vehicle navigation, Kalman filtering, automotive applications and the control of satellite systems.

Darko Vrečko received his Ph.D. from the Faculty of Electrical Engineering, University of Ljubljana. He is a senior research associate at the Department of Systems and Control, Jožef Stefan Institute. His research interests include control, simulation and modelling of various processes such as wastewater treatment plants, fuel cell systems, buildings, production processes, processes with long time delay, etc. He is a co-author of several papers in international journals, chapters in monographs and conference papers.

Jure Knez made his Ph.D. thesis in 2002 at Faculty of Mechanical Engineering on vibration measurement of turbo-generators. Since 2000 he is the lead engineer and co-owner at Dewesoft company, providing total solutions in field of test and measurement. Dewesoft software and solutions is today used in virtually all automotive and aerospace companies for development measurements, in power distribution, industrial and civil engineering applications.

Sašo Blažič received the B.Sc., M. Sc., and Ph. D. degrees in 1996, 1999, and 2002, respectively, from the Faculty of Electrical Engineering, University of Ljubljana. He is currently a Professor with the University of Ljubljana, Faculty of Electrical Engineering. His research interests include adaptive, fuzzy and predictive control of dynamical systems and modelling of nonlinear systems. Recently, the focus of his research has moved towards the areas of autonomous mobile systems, mobile robotics, and the control of satellite systems. He is the author or co-author of 47 journal papers (among those 28 in journals with impact factor), four chapters in the edited books, two patent applications, and numerous conference papers. From 2010 Sašo Blažič has served as a president of the Automatic control society of Slovenia (a member of the IFAC).

AUTHORS' ADDRESSES

Rok Juhant,
Jure Knez,
Dewesoft d.o.o
Gabrsko 11a, 1240 Trbovlje, Slovenia
email: rok.juhant@gmail.com, jure.knez@dewesoft.com

Darko Vrečko,
Department of Systems and Control,
Jožef Stefan Institute,
Jamova 39, SI-1000 Ljubljana, Slovenia
email: darko.vrecko@ijs.si

Sašo Blažič,
University of Ljubljana, Faculty of Electrical Engineering,
Tržaška cesta 25, 1000 Ljubljana, Slovenia
email: saso.blazic@fe.uni-lj.si

Received: 2014-10-13
Accepted: 2014-11-25